Journal Name

ARTICLE

Synthesis of bright red-emissive dicyanoetheno-bridged hexa-*peri*-hexabenzocoronene dimers

Received 00th January 20xx,
Accepted 00th January 20xx

DOI: 10.1039/x0xx00000x

www.rsc.org/

Kazuma Oda,[a] Satoru Hiroto,[a]* Ichiro Hisaki[b] and Hiroshi Shinokubo[a]*

Introduction of a dicyanomethyl anion group to hexa-*peri*-hexabenzocoronene (HBC) substantially enhanced the emission property of HBC due to large perturbation of its electronic structure. In addition, dicyanoetheno-bridged HBC dimers obtained from oxidation of a dicyanomethyl HBC anion exhibited bright red emission in solution and solid states. Intramolecular charge transfer interactions between the HBC units and the dicyanoethene bridge induced solvatochromic behaviour in their emission spectra. Dicyanoetheno-bridged HBC dimers exhibited *cis*–*trans* photoisomerization behaviour in the solution, affording the mixture in *cis*-isomer dominance at the photostationary state. Theoretical calculations revealed that the *cis*-isomer is more thermodynamically stable than the *trans*-isomer.

Introduction

Polycyclic aromatic hydrocarbons (PAHs), small fragments of graphenes, have attracted significant attentions as optical and electronic molecular materials.[1] Among a large number of PAHs, hexa-*peri*-hexabenzocoronenes (HBCs) have been regarded as a good model for a small piece of armchair-edged graphenes. HBCs have been investigated as a centrepiece in supramolecular chemistry because of their disk-like large π-conjugated planes, promoting efficient intermolecular π–π interaction.[2] In addition, HBCs have rich electronic properties, which would be applicable to semiconducting materials such as *p*-type field-effect transistor (FET) owing to their electron-donating nature.[3] On the other hand, HBCs usually have poor optical characteristics due to their highly symmetrical structures, which induce symmetry-forbidden transition from the S_1 to the ground state S_0.[4] Furthermore, the large and planar π-surface of HBCs prompts aggregation-caused fluorescence quenching (ACQ), resulting in low emission efficiency. In contrast to these situations, nanometre-sized carbon quantum dots, so-called nanographenes, have been investigated as emissive materials for the application to optical devices.[5] Thus, it is important to establish a methodology to tune emissive properties of HBCs, which leads to highly emissive carbon quantum dots.

Introduction of functionalities at HBC peripheries causes perturbation of their electronic structures and dynamic behaviour.[6] Such electronic perturbation can modulate their optical properties. We have recently developed regioselective functionalizations of HBCs through iridium catalysed direct C–H borylation.[4b, 7] Installation of electron-donating and withdrawing groups at HBC peripheries enhanced the fluorescence quantum yields. For example, amino-substituted HBCs exhibited relatively strong fluorescence in the solution state. However, amino-HBCs were not very stable under aerobic conditions. In addition, solid-state emissive HBCs have never been achieved.

A dicyanoethene unit is a useful component to allow effective construction of donor–acceptor–donor (D-A-D) chromophores.[8] Such chromophores exhibit non-linear optical properties derived from their strong polarizability.[9] For instance, 2,3-bis[4-(diphenylamino)phenyl]fumaronitrile (NPAFN) (Fig. 1), has been widely used as a non-doped host emitters for red organic light-emitting diodes and aggregation induced emission (AIE) fluorophore.[10] Here we report the serendipitous synthesis of dicyanoetheno-bridged HBC dimers by oxidation of a dicyanomethyl HBC anion. Because of the D–A–D type electronic structure, dicyanoetheno-bridged HBC dimers exhibited bright red emission in solution and solid states.

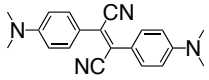

NPAFN

Fig. 1 Structure of 2,3-bis[4-(diphenylamino)phenyl]fumaronitrile (NPAFN).

Results and discussion

Scheme 1 illustrates the synthesis of dicyanomethyl HBC **4**. Iridium-catalysed direct borylation of pentamesityl substituted

[a] *Department of Applied Chemistry, Graduate School of Engineering, Nagoya University, Aichi, 464-8603, Japan. E-mail: hshino@apchem.nagoya-u.ac.jp, hiroto@apchem.nagoya-u.ac.jp; Fax: (+81)-52-789-5113*
[b] *Department of Material and Life Science, Division of Advanced Science and Biotechnology, Graduate School of Engineering, Osaka University, Osaka, 565-0871, Japan. E-mail: hisaki@mls.eng.osaka-u.ac.jp; Fax: (+81)-6-6879-7406*

†Electronic Supplementary Information (ESI) available: ^{1}H NMR and ^{13}C NMR spectra for all compounds, and optical properties of **4**, **5a** and **5b**, and theoretical calculations. See DOI: 10.1039/x0xx00000x

HBC **1** proceeded smoothly in THF, producing monoborylated product **2** in 90%.[4b,11] Monoborylated HBC **2** was easily converted to monoiodo HBC **3** in 78% by treatment of copper(I) iodide (1.5 equiv) and *N*-iodosuccinimide (1.5 equiv) in a mixture of DMF/toluene (2:1, *v/v*).[12] Subsequently, dicyanomethyl HBC **4** was obtained in 78% by Takahashi coupling of **3** with malononitrile (3.6 equiv) in the presence of $Pd(PPh_3)_4$ (30 mol%), copper(I) iodide (1.1 equiv) and sodium *tert*-butoxide (4.1 equiv) in THF.[13] Dicyanomethyl HBC **4** was stable in the solid state but relatively sensitive to air in solution. Introduction of a dicyanomethyl group was confirmed by NMR analysis. The ^{1}H NMR spectrum of **4** exhibited a single peak at 5.62 ppm due to a methine proton of a dicyanomethyl substituent.

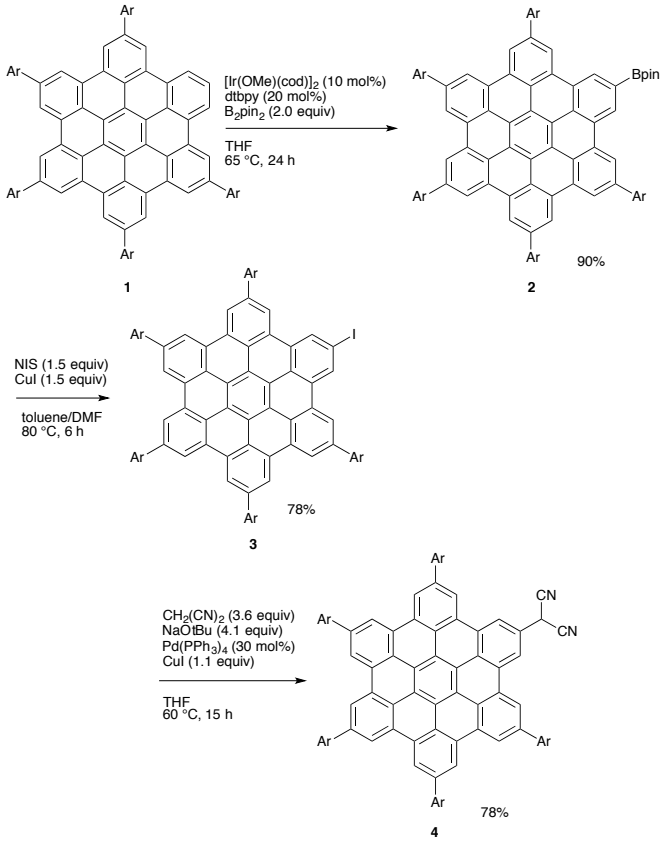

Scheme 1. Synthesis of dicyanomethyl HBC **4**. Ar = mesityl, dtbpy = 4,4'-Di-*tert*-butyl-2,2'-bipyridyl.

A dicyanomethyl group has a highly acidic proton. Treatment of **4** with tetrabutylammonium hydroxide followed by reprecipitation by addition of water provided a salt **4**$^-$**[TBA**$^+$**]** as an orange solid.[14] **4**$^-$**[TBA**$^+$**]** was stable enough to be handled with under aerobic conditions. The generation of the anionic specie **4**$^-$**[TBA**$^+$**]** was monitored by NMR analysis: the methylene proton of **4** around 5 ppm disappeared upon addition of tetrabutylammonium hydroxide.

The dicyanomethyl anion was easily oxidized chemically and electronically due to its electron-rich nature. We anticipated that the large π-conjugation system of the HBC core would enhance the stability of the oxidized intermediate. We then attempted to oxidize **4**$^-$**[TBA**$^+$**]**. Treatment of **4**$^-$**[TBA**$^+$**]** with an excess amount of PbO_2 afforded two red colored compounds **5a** and **5b** (Scheme 2). These compounds were separable by silica-gel column chromatography under careful light shielding. Both compounds showed the same mass spectrum (*m/z* = 2301.0650 for **5a**, *m/z* = 2301.0659 for **5b**). The isotopic patterns of their high-resolution mass spectra were in good agreement with the component of $[C_{178}H_{134}N_2]^+$. Further characterization of **5a** and **5b** were carried out by NMR spectroscopy. ^{1}H NMR spectra of both compounds suggested their highly symmetric feature. The ^{13}C NMR spectrum of **5a** showed 36 peaks around 110–150 ppm due to 34 aromatic, one alkenyl, and one cyano carbon atoms (Fig. S14). While a singlet peak at 29.3 ppm was observed due to methine sp^3 carbon of the dicyanomethyl group in the ^{13}C NMR spectrum of **4** (Fig. S10), **5a** and **5b** showed no sp^3 carbon peak except methyl groups, suggesting the transformation of the dicyanomethyl unit. On the basis of these analyses, we characterized the compound **5a** and **5b** as dicyanoetheno-linked HBC dimers. The peaks of HBC units in the ^{1}H NMR spectrum of **5b** appeared in the same region as those of **4** (Fig. S15). On the other hand, two peaks due to the HBC units and mesityl aromatic protons were observed in the higher field (8.47 and 6.48 ppm) in the case of **5a** (Fig. S13). These shifts in **5a** indicated the presence of the shielding effect by the ring current of the other HBC unit. To reveal conformations of these compounds in the solution state, ^{1}H–^{1}H ROESY NMR experiments for **5b** and **5a** were conducted. For **5a**, all protons of the HBC cores were fully assigned on the basis of ^{1}H–^{1}H correlation between protons at the HBC periphery and *ortho* methyl protons of mesityl groups (Fig. 2, S19): there were ^{1}H–^{1}H correlations between H_{pa} (2.03 ppm) at *para* position, and H_c (8.77 ppm) and H_d (8.86 ppm) of the HBC unit (Fig. 2). On the other hand, methyl protons of mesityl *para*-position showed no correlation with HBC protons in **5b**. These analyses concluded that **5a** and **5b** are *cis* and *trans* isomers, respectively.

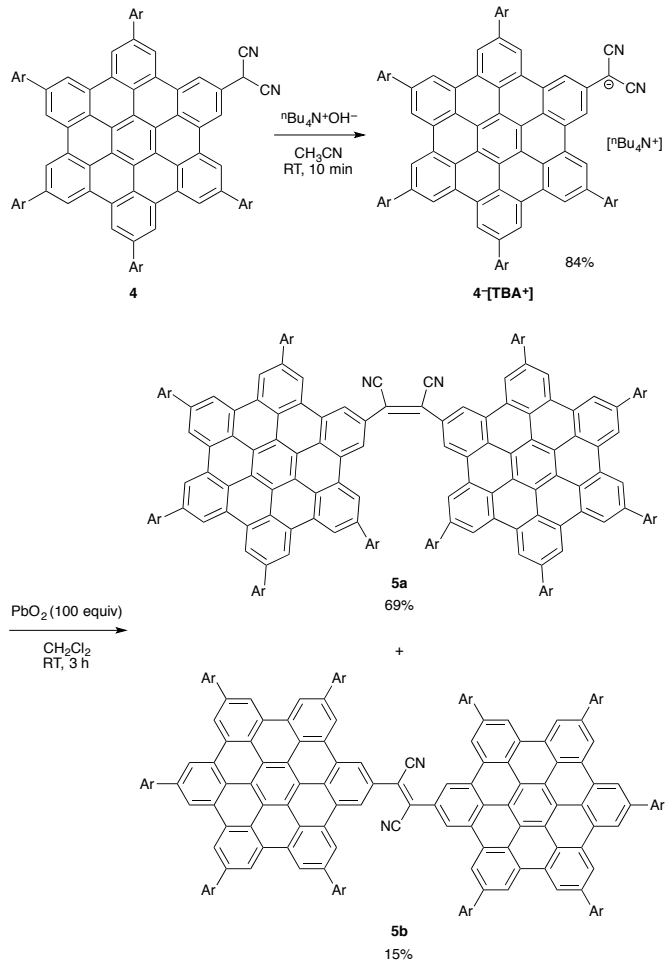

Scheme 2. Deprotonation followed by oxidative dimerization of **4**.

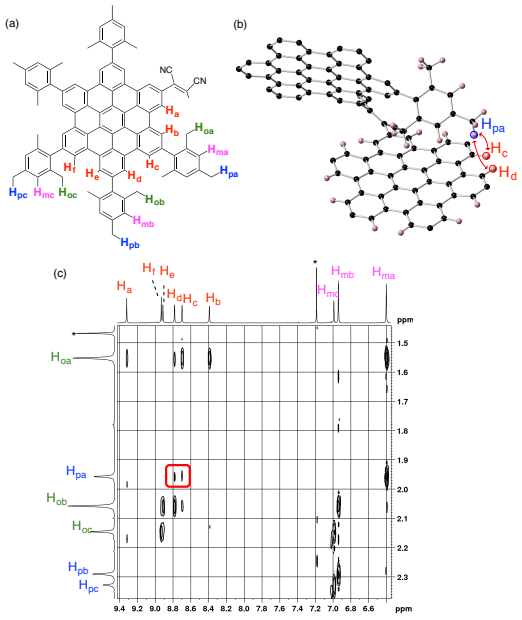

Fig. 2 (a) Labeling of protons in **5a**, (b) ^{1}H–^{1}H correlations between H_{pa} at *para* position and H_c and H_d of the HBC unit, and (c) ^{1}H–^{1}H ROESY NMR spectrum of **5a** in $CDCl_3$.

The structures of **5a** and **5b** were unambiguously elucidated by X-ray diffraction analysis (Fig. 3).[15] The ethene unit in **5a** takes *cis* conformation and one of the HBC cores partially overlaps with the other one. This result is consistent with (well described) the two upfield-shifted peaks observed in the ^{1}H NMR spectrum of **5a**. The dihedral angle between two HBC planes of **5a** was 38.44°. The average torsion angle between the HBC and the central dicyanoethene units was 36.95°. The bond length of the central C–C double bond of **5a** was 1.342(8) Å, which is comparable with typical sp^2–sp^2 C–C bond lengths (1.34 Å) and fumaronitrile derivatives (1.34–1.36 Å).[10c, 16] The averaged distance between *para*-methyl carbon atoms in mesityl groups and the HBC surfaces was 3.345 Å, indicating the presence of the CH–π interactions. The ethene unit of **5b** adopts *trans* conformation, in which each HBC unit points to the opposite direction. The dihedral angle between the two HBC planes was 0.0°. The central dicyanoethene unit was tilted to the HBC planes due to the steric repulsion between the cyano group and HBC core.[10c] The average tilting angle between the HBC and central dicyanoethene units was 46.79°, which were larger than that of **5a**. The bond length of the central C–C double bond of **5b** was 1.343(6) Å, which is similar with that of **5a**.

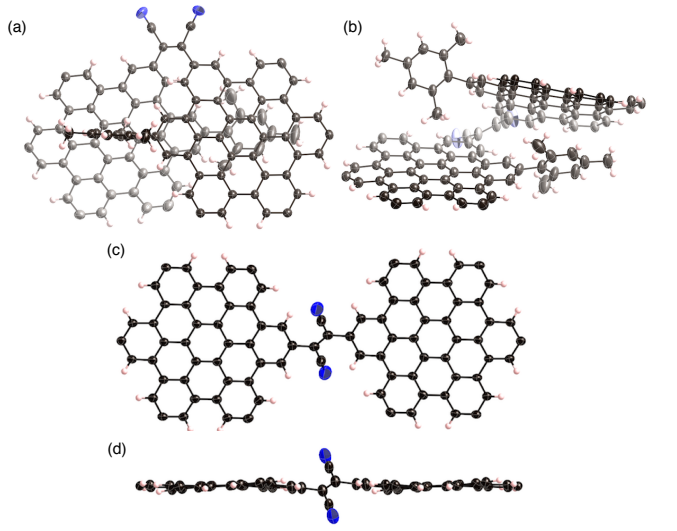

Fig. 3 X-ray crystal structures of **5a** and **5b**. (a) Top view and (b) side view of **5a**. (c) Top view and (d) side view of **5b**. Mesityl groups except for the internal ones are omitted for clarity in (a) and (b), and all mesityl groups are omitted for clarity in (c) and (d). The thermal ellipsoids were scaled at the 50% probability level.

The structures of **5a** and **5b** in gaseous phase were calculated by density functional theory (DFT) method (Fig. S27). The geometries were optimized by the ONIOM method using a combination of a density functional theory at the B3LYP/6-31G(d) level for HBC cores and the semi-empirical PM6 method for mesityl groups. As a result, almost the same structures were elucidated, indicating that the folded structure of **5a** is not influenced by crystal packing. The thermal energy of **5a** was lower than that of **5b** by 6.61 kJ/mol, suggesting the dominance of the *cis*-conformation (Table S3).

Next, we investigated the reaction mechanism of the dimerization reaction. We discovered that oxidation of **4$^-$[TBA$^+$]** with PbO_2 afforded a non-emissive compound in addition to the starting material **4** after 20 min. After additional 40 min, this compound almost disappeared and the

spots of **5a** and **5b** were detected by TLC and ^{1}H NMR analysis of the crude product. These results indicated that this non-emissive compound is an intermediate for the generation of **5a** and **5b**. This non-emissive compound **6** was purified by silica-gel column chromatography, and characterized by NMR and HR-MS analysis. The ^{13}C NMR spectrum of the neutral precursor **4** exhibited a single peak at 29.3 ppm due to methine sp^3 carbon of dicyanomethyl groups, while that of **6** showed a single peak at 55.8 ppm, suggesting the bond formation between dicyanomethyl units (Fig. S18). HR-MS analysis showed the parent ion peak at *m/z* = 2353.0620, which was consistent with the exact mass of tetracyanoethylene-linked HBC dimer **6**. Recently, Sakamaki and Seki reported that a dicyanomethyl group is oxidized to afford dicyanomethyl radical species, which undergoes effective dimerization.[13] In fact, treatment of dicyanomethyl HBC **4** with an excess amount of PbO_2 in dichloromethane afforded **6** in 75% yield (Scheme S1). **6** was converted to **5a** and **5b** in 55% and 13% yields, respectively, by treatment with sodium hydroxide (10 equiv) in the presence of tetrabutylammonium bromide (10 equiv) for 10 h in dichloromethane at room temperature (Scheme 3). In this case, no reaction proceeded in the absence of tetrabutylammonium bromide due to insolubility of sodium hydroxide, suggesting that tetrabutylammonium ion in **4$^-$[TBA$^+$]** worked as a phase transfer catalyst. According to these results, we propose the reaction mechanism for the generation of dicyanoetheno HBC **5a** and **5b** in Scheme 4.[17] First, nucleophilic attack of a hydroxy ion on the nitrile carbon followed by a C–C bond cleavage affords carbanion species. Subsequently, generation of C–C double bond by an elimination of a cyanide ion provides the dicyanoethene moiety.

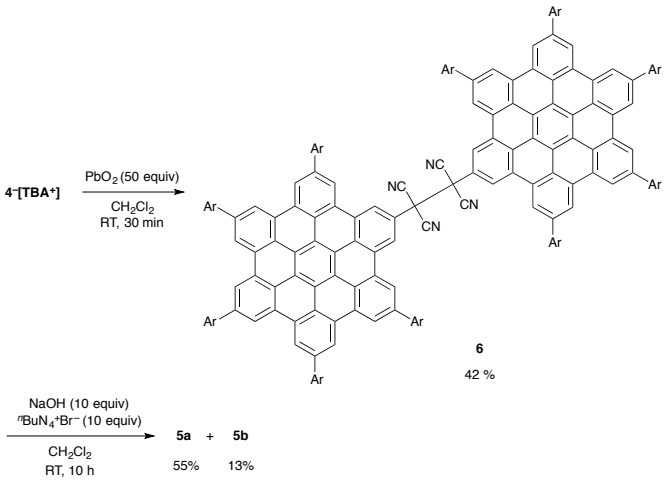

Scheme 3. Generation and base-mediated decyanation of tetracyanoethylene-bridged HBC dimer **6**.

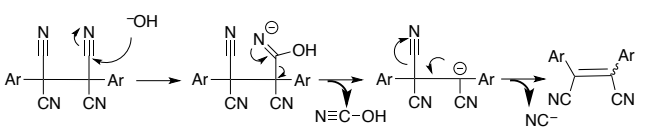

Scheme 4. Proposed reaction mechanism for the generation of dicyanoetheno-bridged HBC dimer.

HBC dimers **5a** and **5b** underwent photoisomerization in solution under room light.[18] ^{1}H NMR analysis revealed that pure **5b** in $CDCl_3$ was changed to a mixture of **5a** and **5b** (**5a**:**5b** = 83:17) after 8 h under room light without light shielding (Fig. S24). A mixture of **5a** and **5b** (**5a**:**5b** = 82:18) was also obtained from **5a** under the same conditions (Fig. S25). In contrast, the spectrum of **5a** remained unchanged after 8 h under dark. These results clearly indicate that *cis–trans* isomerization occurred by irradiation of room light. The ratio of **5a** to **5b** at the photostationary state (PPS) was dependent on the temperature in light irradiation. The ratio of **5a** decreased as the irradiation temperature decreased (Table 1, Fig. S26).[18b, 19]

Table 1. The ratio of **5a** at PPS depending on the irradiation temperatures

Temperature for irradiation (°C)	Yield of **5a** at PSS (%)
90	94
26	87
–78	78

Deprotonation of **4** caused dramatic change of optical properties. A broad absorption band around 500 nm was observed for the salt **4$^-$[TBA$^+$]** (Fig. 4a). In addition, **4$^-$[TBA$^+$]** exhibited bright orange fluorescence (617 nm, Φ_f = 0.24) in dichloromethane, while precursor **4** showed weak green emission (472 nm, Φ_f = 0.04) (Fig. 4b).

A significant change was also observed in the absorption spectra of dicyanoetheno-bridged dimers. In the UV-vis absorption spectra of **5a** and **5b** in dichloromethane, a new absorption band appeared around 480 nm, which was not observed in the spectrum of **4** (Fig. 5a). The lowest energy absorption band of **5a** (λ_{max} = 483 nm) was red-shifted in comparison to that of **5b** (λ_{max} = 478 nm). This result is in good agreement with the calculated absorption energies of **5a** and **5b** by the TD-DFT calculations as discussed later (Fig. S28). During the measurement, no change in the absorption spectra of **5a** and **5b** were observed, indicating the enhanced photostability of these compounds due to the electron-withdrawing dicyanoethene unit.

HBC dimers **5a** and **5b** also exhibited red fluorescence in the solution state (Fig. 5b). To further investigate these optical features, emission spectra of the **5a** and **5b** were measured in various solvents (Fig. 5c, Fig. S22). The maximum emission peaks of **5a** showed bathochromic shift as the solvent polarity increased: cyclohexane (619 nm, Φ_f = 0.21), toluene (629 nm, Φ_f = 0.25), ethyl acetate (680 nm, Φ_f = 0.12), dichloroethane (717 nm, Φ_f = 0.08), and acetone (739 nm, Φ_f = 0.04). The emission wavelength of **5b** exhibited bathochromic shift depending on solvent polarities in similar fashion with that of **5a**. These solvent effects of **5a** and **5b** indicated that both of **5a** and **5b** has intramolecular charge transfer character. Notably, **5a** and **5b** showed red fluorescence in the solid state

(Fig. 5d, **5a**: 687 nm, Φ_f = 0.18, **5b**: 666 nm, Φ_f = 0.21, using a drop-cast film from a dichloromethane solution deposited onto a quartz substrate). According to the absorption spectra for the film of **5a** and **5b** (Fig. S21), Stokes shifts of **5a** and **5b** were 6105 cm^{-1} and 4985 cm^{-1}, respectively, which were remarkably larger than parent HBC **4** (181 cm^{-1}). These large Stokes shifts due to intramolecular charge transfer inhibit self-absorption quenching, enhancing fluorescence quantum yield in solid state.[20]

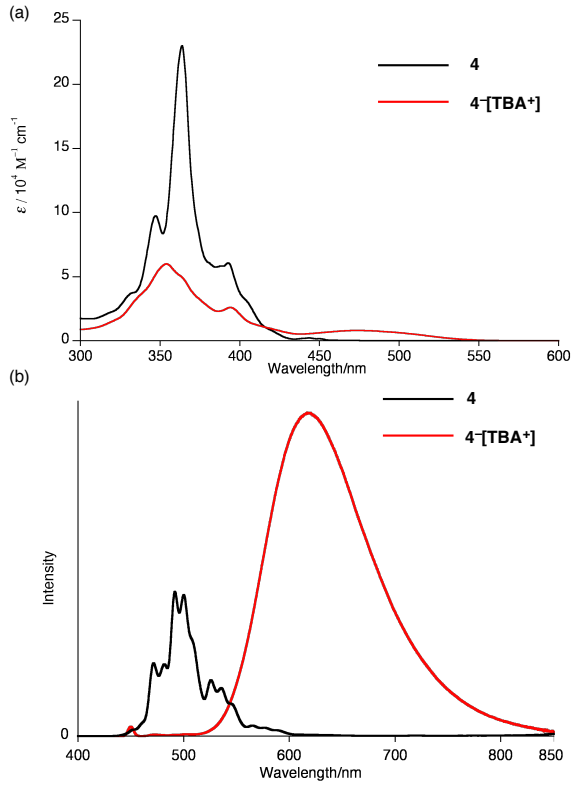

Fig. 4 (a) UV-vis absorption spectra and (b) fluorescence spectra of **4** and anion **4**$^-$**[TBA**$^+$**]** in dichloromethane upon excitation at 350 and 450 nm, respectively. Each emission spectrum was obtained at the concentration of 1 μM.

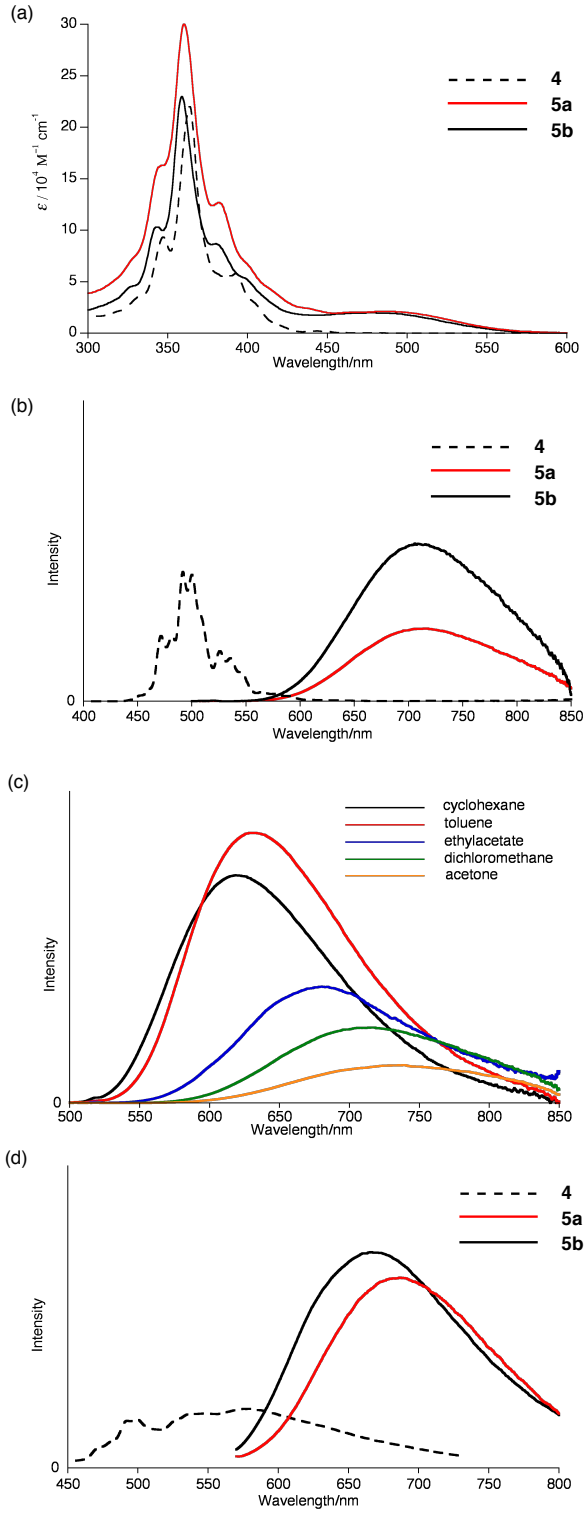

Fig. 5 (a) UV-vis absorption spectra and (b) emission spectra of **5a**, **5b** and **4** in CH_2Cl_2. (c) Emission spectra of **5a** in various solvents. (d) Emission spectra of **5a**, **5b** and **4** in the drop-cast film. Excitation wavelength: 360 nm for **4**, 450 nm for **5a** and **5b**.

Fluorescence decay measurements were performed to reveal excited-state behaviour. Fluorescence lifetimes of **5a** and **5b** in dichloromethane were determined to be 5.5 and 4.8 ns, respectively, with single-exponential decay, which were shorter than that of monomer **4** (19.4 ns) (Table 2). The short

lifetimes for **5a** and **5b** reflected the existence of dynamic behaviour in excited state. Non-radiative constants k_{nr} of **5a** and **5b** calculated from fluorescence lifetime and quantum yields were larger than that of **4** indicated the flexible geometries for **5a** and **5b**. In addition, we have measured lifetimes of the 1wt% doped films of **5a** and **5b** in poly vinyl chloride (PVC). For **5b**, almost the same fluorescence quantum yields and lifetimes in the solid state were observed in comparison to that in the solution state. On the other hand, fluorescence quantum yields of **5a** in the solid and film states were higher than that in the solution state (Table S1). These results indicated the flexible nature of **5a** as compared with **5b**.

Table 2. Fluorescence parameters of **4**, **5a** and **5b**.

Compounds	τ (ns)	Φ_f	k_f (10^7 s^{-1})	k_{nr} (10^7 s^{-1})
4	19.4	0.04	0.21	4.9
5a	5.5	0.08	1.5	17
5b	4.8	0.17	3.5	17

The molecular orbitals of **5a** and **5b** calculated at the B3LYP/6-31G(d) level revealed that HOMOs were localized on the HBC skeleton, while LUMOs located mainly on the dicyanoethene moiety due to the electron deficient nature of cyano groups (Fig. 6). These calculations indicated the intramolecular charge transfer character for **5a** and **5b** from the electron-rich HBC core to the electron-deficient dicyanoethene moiety. On the basis of TD-DFT calculations, the lowest energy absorption bands of **5a** and **5b** were assigned to intramolecular charge transfer transition, resulting in bathochromic-shift as compared with **4.**

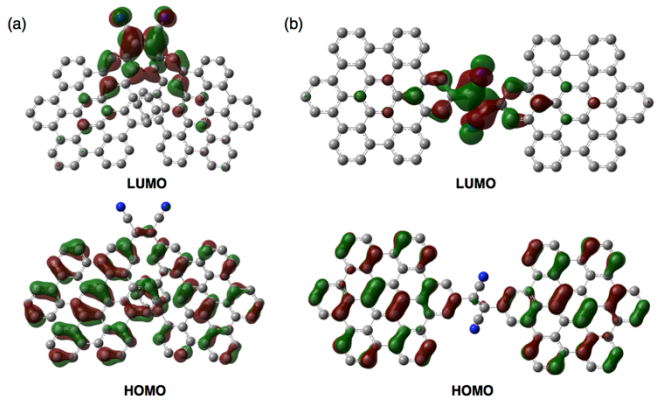

Fig. 6 Frontier molecular orbitals of a) **5a** and b) **5b** calculated at the B3LYP/6-31G(d) level.

Conclusions

In conclusion, we have succeeded in the efficient synthesis of *cis*- and *trans*-dicyanoetheno-bridged HBC dimers through oxidation of a dicyanomethyl HBC anion. Dicyanotheno-bridged HBC dimers exhibited *cis*–*trans* photoisomerization behaviour in solution. X-ray diffraction analysis and theoretical calculations revealed that the *cis* isomer is more thermodynamically stable than the *trans* isomer. Intramolecular charge transfer interactions from the HBC cores to electron-deficient dicyanoethene bridge induced solvatochromic behaviour in emission spectra of the dimers. Such electronic deviation of HBC cores enabled allowed S_1–S_0 transition, exhibiting bright red emission both in solution and solid states. These results suggest that introduction of dicyanomethyl- and dicyanoetheno-unit offers rich optical properties to a variety of carbon materials such as graphene quantum dots. Further application of our protocol to larger carbon materials has been under investigation.

Experimental Section

Instrumental and materials

^{1}H NMR (500 MHz) and ^{13}C NMR (126 MHz) spectra were recorded on a Bruker AVANCE III HD spectrometer, and chemical shifts were reported as the delta scale in ppm relative to $CHCl_3$ (d = 7.260 ppm) and CD_3CN (d = 1.94 ppm) for ^{1}H NMR and $CDCl_3$ (d = 77.16 ppm) and CD_3CN (d = 118.26 ppm) for ^{13}C NMR. UV/vis/NIR absorption spectra were recorded on a Shimadzu UV-2550. Emission spectra were recorded on a JASCO FP-6500 spectrometer and absolute fluorescence quantum yields were measured by photon-counting method using an integration sphere. Fluorescence lifetimes were recorded on a Hamamatsu Photonics Quantaurus-tau (C11367-25). High-Resolution (HR) Mass spectra were recorded on a Bruker microTOF using positive mode ESI method for acetonitrile solutions. X-ray diffraction data of **5a** was taken on a Rigaku CCD diffractometer (Saturn 724 with MicroMax-007) with Varimax Mo optics using graphite monochromated MoKα radiation (λ = 0.71075 Å). X-ray diffraction data for **5b** was collected using synchrotron radiation (λ = 0.8000 Å) at BL38B1 in the Spring-8 with approval of the Japan Synchrotron Radiation Research Institute (JASRI) (proposal No. 2016B1151). The oscillation angle and camera distance were 2° and 75 mm, respectively. The exposure time per frame was 20s or 40s depending on the data set. Two data sets consisted of 90 frames were integrated, scaled, and merged with the programs HKL2000. Unless otherwise noted, materials obtained from commercial suppliers were used without further purification.

2,5,8,11,14-Pentamesitylhexabenzo[*bc*,*ef*,*hi*,*kl*,*no*,*qr*]coronene (1).

A solution of $FeCl_3$ (1.98 g, 12.2 mmol) in CH_3NO_2 (4.0 mL) was added to a solution of 1,2,3,4,5-pentakis(4-mesitylphenyl)-6-phenylbenzene **7** (676 mg, 0.600 mmol) in anhydrous CH_2Cl_2/EtOH (100 mL/0.05 mL). The reaction mixture was stirred for 1 h with continuous N_2 bubbling through the reaction mixture. The reaction mixture was poured into MeOH and concentrated in vacuo. Purification of the residue by column chromatography on silica-gel (CH_2Cl_2) followed by recrystallization from CH_2Cl_2/MeOH afforded **1** (606 mg, 0.544 mmol) in 91% yield. ^{1}H NMR ($CDCl_3$): d 9.24 (d, J = 8.0 Hz, 2H, HBC), 9.12 (s, J = 8.0 Hz, 2H, HBC), 9.03 (s, 8H, HBC), 8.22 (t, J = 8.0 Hz, 1H, HBC), 7.14 (s, 4H, Mes), 7.09 (s, 6H, Mes), 2.46 (s,

6H, *p*-Me), 2.43 (s, 9H, *p*-Me), and 2.24-2.27 (s+s+s, 30H, *o*-Me) ppm; ^{13}C NMR ($CDCl_3$): *d* 140.2, 140.2, 140.1, 139.4, 139.2, 137.4, 137.3, 136.5, 136.3, 131.1, 131.1, 131.0, 128.6, 127.3, 126.1, 124.7, 124.6, 123.7, 123.7, 123.6, 122.5, 121.6, 121.5, 121.4, 21.5, 21.3, and 21.3 ppm; HR-MS (ESI-MS): *m/z* = 1113.5408, calcd for $(C_{87}H_{69})^+$ = 1113.5394 [$(M + H)^+$].

2-Bolyl-5,8,11,14,17-pentamesitylhexabenzo[*bc*,*ef*,*hi*,*kl*,*no*,*qr*]coronene(s) (2).

A Schlenk flask containing **1** (333 mg, 0.299 mmol), bis(pinacolato)diboron (152.8 mg, 0.602 mmol), 4,4'-di-*tert*-butyl-2,2'-bipyridyl (17.4 mg, 0.0648 mmol), and $[Ir(OMe)(cod)]_2$ (19.95 mg, 0.0301 mmol) was purged with N_2, and then charged with anhydrous and degassed THF (15 mL) and mixture was stirred for 24 h at 65 °C. The solvent was removed in vacuo, and purification of the residue by column chromatography on silica-gel followed by recrystallization from $CHCl_3$/MeOH afforded 2-bolyl-5,8,11,14,17-pentamesitylhexabenzo[*bc*,*ef*,*hi*,*kl*,*no*,*qr*]coronene **2** (334.6 mg, 0.270 mmol) in 78% yield. ^{1}H NMR ($CDCl_3$): *d* 9.66 (s, 2H, HBC), 9.23 (s, 2H, HBC), 9.02 (s, 8H, HBC), 7.16 (s, 4H, Mes), 7.08 (s, 6H, Mes), 2.42-2.48 (s+s, 15H, *p*-Me), 2.23-2.26 (s+s, 30H, *o*-Me), and 1.52 (s, 12H, Bpin) ppm; ^{13}C NMR ($CDCl_3$): *d* 140.2, 140.2, 140.2, 139.5, 139.2, 139.2, 137.4, 137.2, 136.6, 136.3, 131.4, 131.2, 131.1, 130.0, 128.8, 128.0, 124.6, 123.7, 123.7, 123.4, 122.0, 121.8, 121.4, 121.3, 84.6, 25.2, 21.5, 21.5, 21.3, and 21.3 ppm; HR-MS (ESI-MS): *m/z* = 1239.6309, calcd for $(C_{93}H_{80}BO_2)^+$ = 1239.6251 [$(M + H)^+$].

2-Iodo-5, 8, 11, 14, 17-pentamesitylhexabenzo[*bc*,*ef*,*hi*,*kl*,*no*,*qr*]coronene (3).

To a round-bottom flask containing 2-bolyl-5,8,11,14,17-pentamesitylhexabenzo[*bc*,*ef*,*hi*,*kl*,*no*,*qr*]coronene (185.7 mg, 0.150 mmol), copper(I) iodide (42.1 mg, 0.221 mmol), and *N*-iodo succinimide (49.9 mg, 0.222 mmol) was added DMF/toluene (10 mL/5 mL) and the mixture was stirred for 6 h at 80 °C under light shielding. The reaction was quenched with aqueous sodium thiosulfate, and the mixture was extracted with EtOAc. The organic layer was washed with water, dried over anhydrous Na_2SO_4, and concentrated in vacuo. Purification of the residue by column chromatography on silica-gel (CH_2Cl_2) followed by recrystallization from CH_2Cl_2/MeOH afforded 2-iodo-5,8,11,14,17-pentamesitylhexabenzo[*bc*,*ef*,*hi*,*kl*,*no*,*qr*]coronene 2 (145.7 mg, 0.118 mmol) in 78% yield. ^{1}H NMR ($CDCl_3$): *d* 9.49 (s, 2H, HBC), 9.00-9.05 (s+s+s, 10H, HBC), 7.14 (s, 4H, Mes), 7.09 (s, 6H, Mes), 2.42-2.46 (s+s, 15H, *p*-Me), and 2.23-2.26 (s+s, 30H, *o*-Me) ppm; ^{13}C NMR ($CDCl_3$): *d* 140.4, 140.4, 139.1, 137.5, 137.3, 136.4, 136.2, 132.8, 131.2, 131.1, 131.0, 129.8, 128.6, 128.6, 125.1, 124.7, 124.6, 124.6, 124.2, 123.9, 123.8, 123.8, 123.6, 121.8, 121.5, 21.5, 21.4, 21.3, and 21.3 ppm; HR-MS (ESI-MS): *m/z* = 1239.4389, calcd for $(C_{87}H_{68}I)^+$ = 1239.4360 [$(M + H)^+$].

2-dicyanomethyl-5,8,11,14,17-pentamesitylhexabenzo[*bc*,*ef*,*hi*,*kl*,*no*,*qr*]coronene 4.

A Schlenk flask containing NaO^tBu (27.2 mg, 0.283 mmol) and malononitrile (16.1 mg, 0.244 mmol) was purged with N_2, and then charged with anhydrous and degassed THF (10 mL), and then the resulting mixture was stirred for 15 min at room temperature. To the mixture was added **2** (85.15 mg, 0.0687 mmol), tetrakis(triphenylphosphine)palladium (24.1 mg, 0.0201 mmol), copper(I) iodide (14.4 mg, 0.0756 mmol), and anhydrous and degassed THF (20 mL) at room temperature. The reaction mixture was stirred at 60 °C for 15 h, quenched with aqueous HCl, extracted with CH_2Cl_2, and then dried over Na_2SO_4. The solvent was removed in vacuo, and purification of the residue by column chromatography on silica-gel followed (CH_2Cl_2/hexane) by recrystallization from $CHCl_3$/MeOH afforded 2-dicyanomethyl-5,8,11,14,17-pentamesitylhexabenzo[*bc*,*ef*,*hi*,*kl*,*no*,*qr*]coronene **4** (63.45 mg, 0.0539 mmol) in 78% yield. ^{1}H NMR ($CDCl_3$): *d* 9.26 (s, 2H, HBC), 9.10 (s, 2H, HBC), 9.08 (s, 2H, HBC), 9.04 (s, 6H, HBC), 7.14 (s, 4H, Mes), 7.08 (s, 6H, Mes), 5.62 (s, 1H, $CHCN_2$), 2.42-2.46 (s+s, 15H, *p*-Me), and 2.22-2.26 (s+s, 30H, *o*-Me) ppm; ^{13}C NMR ($CDCl_3$): *d* 140.7, 140.7, 140.6, 139.0, 138.9, 137.7, 137.4, 137.4, 136.4, 136.2, 132.8, 131.4, 131.3, 131.2, 130.9, 129.9, 128.7, 128.6, 124.9, 124.9, 124.9, 124.6, 124.1, 123.9, 123.7, 122.3, 121.7 121.7, 120.6, 120.3, 112.2, 29.3, 21.5, 21.5, 21.4, 21.3, and 21.3 ppm; HR-MS (ESI-MS): *m/z* = 1177.5455, calcd for $(C_{64}H_{69}N_2)^+$ = 1177.5448 [$(M + H)^+$]; UV/vis (CH_2Cl_2): l_{max} (*e* [M^{-1} cm^{-1}]) = 364 (220000), 393 (58000), 444 (2100), and 450 (1600) nm.

2-Dicyanomethyl-5,8,11,14,17-pentamesitylhexabenzo[*bc*,*ef*,*hi*,*kl*,*no*,*qr*]coronene tetrabutylammonium salt ($4^-[TBA^+]$).

A Schlenk tube containing **4** (23.5 mg, 19.9 µmol) was purged with N_2, and charged with anhydrous and degassed CH_3CN (2.0 mL). To the solution, 40% aqueous solution of tetrabutylammonium hydroxide (26.4 mg, 40.7 µmol) was added, and the mixture was stirred at room temperature for 5 min. H_2O was added to the reaction mixture, and precipitation was filtered with H_2O to afford **$4^-[TBA^+]$** (23.9 mg, 166 µmol) in 78% yield. ^{1}H NMR (CD_3CN): *d* 9.09-9.11 (s+s, 8H, HBC), 8.31 (s, 2H, HBC), 8.66 (s, 2H, HBC), 7.12 (s, 4H, Mes), 7.07 (s, 6H, Mes), 2.96 (t, *J* = 8.6 Hz, 8H, $NCH_2C_3H_7$), 2.15 (s, 6H, *p*-Me), 2.37 (s, 3H+6H, *p*-Me), 2.18 (s, 30H, *o*-Me), 1.50 (m, 8H, $NCH_2CH_2C_2H_5$), 1.27 (m, 8H, $NCH_2CH_2CH_2CH_3$), and 0.90 (t, *J* = 7.0 Hz, 12H, $NCH_2CH_2CH_2CH_3$) ppm; ^{13}C NMR (CD_3CN): 141.1, 141.2, 140.2, 140.1, 138.1, 137.8, 137.2, 131.9, 131.9, 131.7, 131.5, 129.3, 129.2, 126.7, 126.6, 124.9, 124.5, 122.2, 120.6, 113.8, 59.3, 59.3, 24.3, 21.5, 21.5, 21.4, 21.3, 21.2, 20.3, and 13.7 ppm.

Synthetic procedure for *cis*- and *trans*-*a,b*-dicyanoetheno HBC dimers

A Schlenk flask containing **$4^-[TBA^+]$** (21.3 mg, 0.0149 mmol) and PbO_2 (360.0 mg, 1.51 mmol) was purged with N_2, and then charged with anhydrous and degassed CH_2Cl_2 (2.0 mL). The resulting mixture was stirred for 3 h at room temperature. The reaction mixture was filtered through Celite with CH_2Cl_2, and concentrated in vacuo. Purification of the residue by column chromatography on silica-gel under careful light shielding followed by recrystallization from $CHCl_3$/MeOH afforded **5a** and **5b** in 69% and 15% yields, respectively. **5a**: R_f = 0.46

(CH_2Cl_2/hexane = 1/1, v/v); ^{1}H NMR ($CDCl_3$): δ 9.39 (s, 4H, HBC), 9.01 (s, 4H, HBC), 8.99 (s, 4H, HBC), 8.86 (s, 4H, HBC), 8.77 (s, 4H, HBC), 8.47 (s, 4H, HBC), 7.07 (s, 4H, Mes), 7.01 (s, 8H, Mes), 6.48 (s, 8H, Mes), 2.40 (s, 6H, *p*-Me), 2.37 (s, 12H, *p*-Me), 2.22 (s, 12H, *p*-Me), 2.13 (s, 24H, *o*-Me), 2.03 (s, 12H, p-Me), and 1.63 (s, 24H, *o*-Me) ppm; ^{13}C NMR ($CDCl_3$): δ 140.7, 140.4, 140.3, 139.0, 138.9, 138.2, 137.4, 137.3, 136.9, 136.2, 136.1, 135.6, 131.6, 131.3, 131.1, 130.9, 130.8, 129.7, 129.1, 128.6, 128.5, 128.1, 127.4, 127.0, 124.5, 124.5, 124.4, 123.9, 123.7, 123.5, 123.0, 122.5, 122.0, 121.5, 120.3, 117.5, 21.5, 21.4, 21.3, 21.2, 21.0, and 20.8 ppm; HR-MS (ESI-MS): *m/z* = 2301.0650, calcd for $(C_{178}H_{135}N_2)^+$ = 2301.0653 [$(M + H)^+$]; UV/vis (CH_2Cl_2): λ_{max} (ε [M^{-1} cm^{-1}]) = 360 (300000), 376 (130000), and 487 (21000) nm; **5b**: R_f = 0.82 (CH_2Cl_2/hexane =1/1, *v/v*); ^{1}H NMR ($CDCl_3$): δ 9.78 (s, 2H, HBC), 9.22 (s, 2H, HBC), 9.11 (s, 2H, HBC), 9.05 (s, 6H, HBC), 7.09–7.10 (s + s, 10H, Mes), 2.41–2.43 (s + s, 15H, *p*-Me), and 2.24–2.29 (s + s, 30H, *o*-Me) ppm; ^{13}C NMR ($CDCl_3$): δ 140.7, 140.7, 140.5, 139.1, 139.0, 137.4, 137.4, 136.4, 136.2, 131.9, 131.3, 131.3, 131.2, 131.0, 130.7, 130.4, 130.2, 128.7, 128.6, 128.4, 128.1, 127.4, 124.9, 124.7, 124.7, 124.0, 123.9, 122.5, 122.4, 122.1, 121.6, 120.6, 117.8, 21.5, 21.5, and 21.3 ppm; HR-MS (ESI-MS): *m/z* = 2301.0659, calcd for $(C_{178}H_{135}N_2)^+$ = 2301.0653 [$(M + H)^+$]; UV/vis (CH_2Cl_2): λ_{max} (ε [M^{-1} cm^{-1}]) = 359 (230000), 375 (88000), and 477 (12000) nm.

1,2-Bis(5,8,11,14,17-pentamesitylhexabenzo[*bc*,*ef*,*hi*,*kl*,*no*,*qr*]coronen-2-yl)ethane-1,1,2,2-tetracarbonitrile (6).

A Schlenk flask containing **4** (13.42 mg, 0.0114 mmol) and PbO_2 was purged with N_2, and then charged with anhydrous and degassed CH_2Cl_2 (2.0 mL). The resulting mixture was stirred for 1 h at room temperature. The reaction mixture was filtered through Celite with CH_2Cl_2, concentrated in vacuo, and purification of the residue by column chromatography on silica-gel followed by recrystallization from CH_2Cl_2/MeOH afforded 1,2-bis(5,8,11,14,17-pentamesitylhexabenzo[*bc*,*ef*,*hi*,*kl*,*no*,*qr*]-coronen-2-yl)ethane-1,1,2,2-tetracarbonitrile **6** (10.10 mg, 4.29 mmol) in 75% yield. ^{1}H NMR ($CDCl_3$): *d*; 9.03 (broad, HBC), and 7.04-7.08 (broad, Mes) ppm; ^{13}C NMR ($CDCl_3$): *d* 140.8, 140.5, 139.0, 138.9, 137.4, 136.2, 136.1, 131.3, 131.3, 130.7, 128.6, 127.6, 125.2, 124.4, 124.0, 122.6, 121.8, 121.6, 119.5, 54.3, 21.5, 21.4, 21.3, and 21.3 ppm; HR-MS (ESI-MS): *m/z* = 2353.0620, calcd for $(C_{180}H_{135}N_4)^+$ = 2353.0715 [$(M + H)^+$].

Acknowledgements

Crystallographic data collection of **5b** was performed at the BL38B1 in the SPring-8 with approval of JASRI (proposal No. 2016B1151). This work was supported by a Grant-in-Aid for Scientific Research on Innovative Areas "New Polymeric Materials Based on Element-Blocks (No.2401)" (JSPS KAKENHI Grant Number 15H00731) and "pi-System Figuration" (No.2601) (JSPS KAKENHI Grant Number JP26102003) and a Grant-in-Aid for Encouragement of Young Scientists (A) (No. 16H06031). S.H. also acknowledges the Asahi Glass Foundation and TOBEMAKI Scholarship Foundation for financial support. K.O. appreciates the JSPS Research Fellowship for Young Scientists.

References

1 (a) U. Beser, M. Kastler, A. Maghsoumi, M. Wagner, C. Castiglioni, M. Tommasini, A. Narita, X. Feng and K. Müllen, *J. Am. Chem. Soc.* 2016, **138**, 4322-4325; (b) P. Hu, S. Lee, T. S. Herng, N. Aratani, T. P. Goncalves, Q. Qi, X. Shi, H. Yamada, K.-W. Huang, J. Ding, D. Kim and J. Wu, *J. Am. Chem. Soc.* 2016, **138**, 1065-1077; (c) J. Cao, G. London, O. Dumele, M. V. W. Rekowski, N. Trapp, L. Ruhlmann, C. Boudon, A. Stanger and F. Diederich, *J. Am. Chem. Soc.* 2015, **137**, 7178-7188; (d) Z. Yao, M. Zhang, H. Wu, L. Yang, R. Li and P. Wang, *J. Am. Chem. Soc.* 2015, **137**, 3799-3802; (e) K. Kawasumi, Q. Zhang, Y. Segawa, L. T. Scott and K. Itami, *Nat. Chem.* 2013, **5**, 739-744; (f) T. M. Figueira-Duarte and K. Müllen, *Chem. Rev.* 2011, **111**, 7260-7314.

2 (a) W. Pisula, X. Feng and K. Müllen, *Adv. Mater.* 2010, **22**, 3634-3649; (b) T. Aida, E. W. Meijer and S. I. Stupp, *Science* 2012, **335**, 813-817.

3 (a) Y. Liu, T. Marszalek, K. Müllen, W. Pisula and X. L. Feng, *Chem. Asian J.* 2016, **11**, 2107-2112; (b) S. S. Babu, S. Prasanthkumar, A. Ajayaghosh, *Angew. Chem. Int. Ed.* 2012, **51**, 1766-1776; (c) W. Pisula, X. Feng and K. Müllen, *Chem. Mater.* 2011, **23**, 554-567; (d) J. Wu, W. Pisula and K. Müllen, *Chem. Rev.* 2007, **107**, 718-747.

4 (a) M. Kastler, J. Schmidt, W. Pisula, D. Sebastiani and K. Müllen, *J. Am. Chem. Soc.* 2006, **128**, 9526-9534; (b) R. Yamaguchi, S. Ito, B. S. Lee, S. Hiroto, D. Kim and H. Shinokubo, *Chem. Asian J.* 2013, **8**, 178-190.

5 L. Li, G. Wu, G. Yang, J. Peng, J. Zhao and J. J. Zhu, *Nanoscale* 2013, **5**, 4015-4039.

6 a)L. Chen, X. Dou, W. Pisula, X. Yang, D. Wu, G. Floudas, X. Feng and K. Müllen, *Chem. Commun.* 2012, **48**, 702-704. b) C. Zhang, Y. Liu, X. Q. Xiong, L. H. Peng, L. Gan, C. F. Chen, H. B. Xu, *Org. Lett.* **2012**, *14*, 5912-5915; c) P. C. Zhu, Y. Liu, L. H. Peng, C. Zhang, *Tetrahedron Lett.* **2014**, *55*, 521-524.

7 R. Yamaguchi, S. Hiroto and H. Shinokubo, *Org. Lett.* 2012, **14**, 2472-2475.

8 (a) F. Bureš, O. Pytela, M. Kivala and F. Diederich, *J. Phys. Org. Chem.* 2011, **24**, 274-281; (b) M. Kivala and F. Diederich, *Acc. Chem. Res.* 2009, **42**, 235-248.

9 M. G. Kuzyk, *J. Mater. Chem.* 2009, **19**, 7444-7465.

10 (a) M. N. Elinson, A. S. Dorofeev, S. K. Feducovich, P. A. Belyakov and G. I. Nikishin, *Eur. J. Org. Chem.* 2007, 3023-3027; (b) H.-C. Yeh, S.-J. Yeh and C.-T. Chen, *Chem. Commun.* 2003, 2632-2633; (c) H.-C. Yeh, W.-C. Wu, Y.-S. Wen, D.-C. Dai, J.-K. Wang and C.-T. Chen, *J. Org. Chem.* 2004, **69**, 6455-6462; (d) K. Li, W. Qin, D. Ding, N. Tomczak, J. Geng, R. Liu, J. Liu, X. Zhang, H. Liu, B. Liu and B. Z. Tang, *Sci. Rep.* 2013, **3**, 1150.

11 D. N. Coventry, A. S. Batsanov, A. E. Goeta, J. A. K. Howard, T. B. Marder and R. N. Perutz, *Chem. Commun.* 2005, 2172-2174.

12 K. Fujimoto, H. Yorimitsu, A. Osuka, *Org. Lett.* 2014, **16**, 972-975.

13 T. Kobashi, D. Sakamaki and S. Seki, *Angew. Chem. Int. Ed.* 2016, *55*, 8634-8638.

14 (a) N. Acton, D. Hou, J. Schwarz and T. J. Katz, *J. Org. Chem.* 1982, **47**, 1011-1018; (b) M. Maxfield, A. N. Bloch and D. O. Cowan, *J. Org. Chem.* 1985, **50**, 1789-1796.

15 Crystallographic data for **5a**: $C_{204}H_{173.84}N_{9.95}O_{2.53}$, *M*w = 2805.03 , triclinic, *P*-1, *a* = 19.0199(8) Å, *b* = 19.4285(8) Å, *c* = 23.4411(8) Å, *α* = 100.927(3)°, *β* = 104.663(3)°, *γ* = 102.902(4)°, *Z* = 2, *R* = 0.1027 (*I* > 2.0 *σ*(*I*)), *R*w = 0.3482 (all

data), GOF = 1.014; Crystallographic data for **5b**: $C_{180}H_{138}C_{12}N_{23}$, *M*w = 2399.99, triclinic, *P*-1, *a* = 12.3105 Å, *b* = 12.6606 Å, *c* = 22.2312 Å, *α* = 84.2590°, *β* = 81.4740°, *γ* = 77.2470°, *Z* = 1, *R* = 0.0997 (*I* > 2.0 *σ*(*I*)), *R*w = 0.3091 (all data), GOF = 1.028; Crystallographic data for **5a** and **5b** has been deposited with the Cambridge Crystallographic Data Centre as supplementary publication no. CCDC-1520193 and CCDC-522906, respectively.

16 C. C. Costain and B. P. Stoicheff, *J. Chem. Phys.* 1959, **30**, 777-782.

17 J.-M. Mattalia, C. M.-Delapierre, H. Hazimeh and M. Chanon, *Arkivoc* 2006, 90-118.

18 (a) A. L. Dobryakov, M. Quick, D. Lenoir, H. Detert, N. P. Ernsting and S. A. Kovalenko, *Chem. Phys. Lett.* 2016, **652**, 225-229; (b) D. H. Waldeck, *Chem. Rev.* 1991, **91**, 415-436.

19 (a) S. Malkin and E. Fischer, *J. Phys. Chem.* 1964, **68**, 1153-1163; (b) S. Malkin and E. Fischer, *J. Phys. Chem.* 1962, **66**, 2482-2486; (c) N. N. M. Sumitani, K. Yoshihara and S. Nagakura, *Chem. Phys. Lett.* 1977, **51**, 183-185.

20 C. H. Zhao, A. Wakamiya, Y. Inukai and S. Yamaguchi, *J. Am. Chem. Soc.* 2006, **128**, 15934-15935.